N95-14475

FATIGUE RELIABILITY METHOD WITH IN-SERVICE INSPECTIONS

H.H. Harkness[1], M. Fleming, B. Moran and T. Belytschko
Robert R. McCormick School of Engineering and Applied Science
Northwestern University, Evanston, Illinois 60208-3109

ABSTRACT

The first order reliability method (FORM) has traditionally been applied in a fatigue reliability setting to one inspection interval at a time, so that the random distribution of crack lengths must be recharacterized following each inspection. The FORM presented here allows each analysis to span several inspection periods without explicit characterization of the crack length distribution upon each inspection. The method thereby preserves the attractive feature of FORM in that relatively few realizations in the random variable space need to be considered. Examples are given which show that the present methodology gives estimates which are in good agreement with Monte Carlo simulations and is efficient even for complex components.

1. Introduction

Probabilistic fatigue methods are often applied in a setting where critical structural components are subjected to crack inspections by non-destructive evaluation (NDE) techniques, so that cracked components can be identified and repaired or replaced. These inspections can significantly reduce the probability of fatigue failure of structures, as well as increase the useful service lives. Quantified measures of reliability (provided by probabilistic methods) allow maximization of these inspection effects through optimization of the inspection schedule. These measures of reliability also allow comparisons of various inspection methods.

A risk analysis methodology for the assessment of structural integrity of aircraft structures has been outlined by Berens et. al. (1991). This methodology which is based on direct integration of probability of failure integrals works extremely well when the number of random variables is relatively small and a single parameter characterization of crack size is adequate. For complicated geometries (involving characterization of three-dimensional crack growth, for example), other modeling techniques such as Monte Carlo simulations (MCS) and the first order reliability method (FORM) are useful for calculating probabilities of failure (see Harkness et. al.(1992) and references therein). Traditionally, these latter techniques have been applied to one inspection interval at a time. However, that approach requires characterization of the crack

[1]Current address; Hibbitt, Karlsson, Sorenson and Associates, Pawtucket, Rhode Island

size distribution (i.e., crack size probability density function) following each inspection, which is costly and difficult. Techniques for recharacterizing crack size distributions at each inspection with FORM are discussed in Rahman and Rice (1992).

An alternative approach is given here which does not require recharacterization of the crack size distribution. The first order reliability method is augmented to account for the effects of the inspections so that the crack size distribution need only be characterized at an initial state. This is of considerable advantage since recharacterizations of the crack length distribution are often tedious or impractical to obtain. In the present work, it is assumed that components with detected cracks are repaired such that their subsequent likelihood of failure is negligible.

In Section 2, the standard FORM and its application to fatigue reliability are reviewed. The introduction of non-destructive evaluation (NDE) into the fatigue reliability problem is discussed in Section 3 along with a description of the augmentation of FORM to efficiently treat multiple inspections. The first part of section 3 is devoted to identifying the quantities of interest in a fatigue reliability analysis with in-service inspections; techniques to evaluate these quantities are given in the remainder of the section. An important aspect of FORM is finding the so-called design points. An algorithm for this task which is applicable to both the standard FORM and the augmented FORM is provided in the Appendix.

Two numerical examples are presented in Section 4. The first example investigates the accuracy of augmented FORM by comparison to MCS results. A more complex fatigue problem is studied in the second example where the MCS approach is not computationally feasible, yet the augmented FORM requires only minutes of CPU time on a workstation. In these examples, the inspection schedule is adjusted so that inspections occur when the probability of failure reaches a specified value. Further discussion and concluding remarks are given in Section 5.

2. FIRST ORDER RELIABILITY METHOD

2.1. Standard Reliability Statement

We begin by defining a performance function, $G(\boldsymbol{x})$, which distinguishes between safe and unsafe realizations of the random variables $\boldsymbol{x}$ (see Fig. 1a). Performance functions are typically defined so that positive outcomes indicate safe realizations and negative outcomes indicate unsafe realizations (the limit case of $G(\boldsymbol{x})=0$ is often included in the failure domain). The objective of a reliability analysis is to determine the probability of failure

$$P_f = P[G(\boldsymbol{x}) \leq 0], \tag{2.1}$$

which is given by

$$P_f = \int_{\Omega_f^x} f_X(\boldsymbol{x})\, d\boldsymbol{x}, \tag{2.2}$$

where Ω_f^x is the failure space ($G(\boldsymbol{x})\leq 0$), and $f_X(\boldsymbol{x})$ is the joint probability density function for realizations in the space of random variables $\boldsymbol{x}$.

The random variables $\boldsymbol{x}$ are often non-normally distributed, making the integral in Eq. (2.2) difficult to evaluate. The random variables $\boldsymbol{x}$ can be mapped to standardized equivalent normal random variables $\boldsymbol{r}$, where each component r_i is an independent Gaussian variable with zero mean and unit variance. This mapping can be achieved via the Rosenblatt transformation (see Rosenblatt 1952; Ang and Tang 1984)

$$r_i = \Phi^{-1}\left[F_i\left(x_i | x_1, x_2, \ldots, x_{i-1}\right)\right], \tag{2.3}$$

where F_i is the conditional cumulative probability at x_i given $x_1, x_2, \ldots, x_{i-1}$. In standardized space, the performance function is transformed to $g(\boldsymbol{r})=G(\boldsymbol{x}(\boldsymbol{r}))$ and Eq. (2.2) becomes

$$P_f = \int_{\Omega_f^r} f_R(\boldsymbol{r})d\boldsymbol{r}, \tag{2.4}$$

where Ω_f^r is the failure space ($g(\boldsymbol{r})\leq 0$) as in Fig. 1b, and $f_R(\boldsymbol{r})$ is the joint probability density function for realizations of random variables $\boldsymbol{r}$. The joint probability density function, $f_R(\boldsymbol{r})$, is simply the product of the probability density functions for all random variables r_i and is given by

$$f_R(\boldsymbol{r}) = \prod_{i=1}^{n} \frac{1}{\sqrt{2\pi}} \exp\left(-\frac{1}{2} r_i^2\right). \tag{2.5}$$

The essence of FORM is to approximate the limit surface $g(\boldsymbol{r})=0$ by a tangent hyperplane at the most likely point of failure, $\boldsymbol{r}_d$. In standard FORM the most likely failure point is the point which minimizes the distance $|\boldsymbol{r}|$ to the failure surface. The resulting "first order" estimate of the probability of failure is then given by

$$P_f^1 = \Phi(-\beta), \tag{2.6}$$

where $\beta=|\mathbf{r}_d|$ and Φ is the standard normal cumulative distribution function. Because the random variables $\mathbf{r}$ are Gaussian, the decay of $f_R(\mathbf{r})$ is exponential and therefore using the closest point provides a good estimat for calculating probability of failure using standard FORM. It will be shown in Section 3.3 that the closest point may not be the most likely failure point when in-service inspections are accounted for.

2.2. Fatigue Reliability

In a fatigue setting, the failure set contains all realizations that result in fatigue lives less than a desired service life, so an appropriate performance function is

$$G(\mathbf{x}) = N_f(\mathbf{x}) - N, \tag{2.7}$$

or in standard Gaussian space

$$g(\mathbf{r}) = N_f(\mathbf{x}(\mathbf{r})) - N, \tag{2.8}$$

where N_f is the fatigue life (which is influenced by several uncertainties) and N is the desired service life. Note that the fatigue life may be defined as the number of cycles for a crack to reach some specified critical size - which may not necessarily correspond to catastrophic failure of the component. Failure is deemed to occur when the fatigue life is shorter than the desired service life ($g<0$). Standard FORM described above is often effective for estimating failure probability versus service life in the absence of inspections or for estimating the probability of failure with inspections when the crack length distribution following an inspection is known. In the latter, a standard FORM analysis is performed for each inspection interval of interest, and the probability of failure is determined in each analysis. This approach requires knowledge of the crack size distribution following each inspection. A more efficient method for treating inspections is introduced in the following Section.

3. FATIGUE RELIABILITY AND IN-SERVICE NDE INSPECTIONS

Consider a fatigue reliability setting where the component is subjected to in-service NDE inspections according to some schedule. The inspection schedule may be prescribed and the failure probabilities sought or conversely, the aim of the analysis may be to determine an inspection schedule which will keep failure probabilities below a specified level. Let N denote the service life (in cycles) and N_I denote the number of

cycles to the inspection prior to N. We seek a method to determine the fatigue reliability (or alternatively failure probability) over the service life, N. As mentioned previously, standard FORM techniques require a complete characterization of the probability density function for the crack size following each inspection. However, an exact determination of the crack size probability density function may be extremely tedious or impractical to obtain especially for cracks in complicated geometries. Rahman and Rice (1992) discuss a method based on the standard FORM itself to recharacterize the crack size distribution at each inspection, but this method may require extensive computations. In the following subsection, we introduce a straightforward and efficient method based on the initial crack size distribution for determining fatigue reliability with NDE inspections, i.e., explicit knowledge of the crack size distribution at each inspection is not required.

3.1. Statement of Reliability Problem with NDE Inspections

The probability of failure is defined here as the probability that the service life of the component exceeds the fatigue life as a result of undetected cracks. Thus the probability of failure, P_f, after N fatigue cycles, can be written as

$$P_f(N) = P[N_f \leq N \mid O_i=0,\ i=1,2,..,I] \tag{3.1}$$

where I is the number of previous inspections at N cycles ($N>N_I$), O_i indicates the outcome of the i-th inspection which is given by:

$$O_i = \begin{cases} 0 & \text{no crack detected } i^{th} \text{ inspection} \\ 1 & \text{crack detected } i^{th} \text{ inspection} \end{cases} \tag{3.2}$$

and N_f is the fatigue life. The outcome of each inspection is random due to uncertainties in the inspection technique and the crack length at the time of the inspection.

Other functions which may be of particular interest can be derived from P_f. The hazard function (or failure rate) $h(N)$ is given by

$$h(N) = \frac{1}{[1-P_f(N)]} \frac{\partial P_f(N)}{\partial N} \tag{3.3}$$

The factor $[1-P_f]$ in Eq. 3.3 is typically very close to unity in a reliability analysis, so the hazard function is effectively equal to the derivative of the probability of failure. Another useful failure probability is the probability of failure since the last inspection (due to an undetected crack), i.e.,

$$P_{fI}(N_s) = P[\, N_I < N_f \leq N \mid O_i = 0,\ i = 1,2,..,I] \tag{3.4}$$

where I is the number of previous inspections at N cycles, and N_I and O_i are as previously defined.

As in the standard FORM the random variable space can be transformed to standardized Gaussian variable space. The probability density function for realizations of $\boldsymbol{r}$ in this space is $f_R(\boldsymbol{r})$ (see Eq. 2.5). To derive an expression for the probability of failure, P_f, at cycle N allowing for NDE inspections, we require the probability density function associated with realizations, $\boldsymbol{r}$, for which the associated cracks are undetected. The probability density function for realizations with undetected cracks after the first I inspections is given by

$$f_U(\boldsymbol{r}) = f_R(\boldsymbol{r}) P_{nd}(\boldsymbol{r},\ N). \tag{3.5}$$

Here, $P_{nd}(\boldsymbol{r}, N)$ is the probability that cracks associated with the realization $\boldsymbol{r}$ are not detected in all of the inspections prior to the current cycle, N, i.e., $P_{nd}(\boldsymbol{r},N) = P[O_i=0$ for $i=1,2,..,I \mid \boldsymbol{r}]$, and is given by

$$P_{nd}(\boldsymbol{r}, N) = \prod_{i=1}^{I} \left\{1 - POD\left[a(\boldsymbol{r}, N_i)\right]\right\} \tag{3.6}$$

where $POD[a(\boldsymbol{r},N_i)]$ is the given probability of detection for the inspection method, and $a(\boldsymbol{r},N_i)$ is the crack length upon the i^{th} inspection for the realization $\boldsymbol{r}$.

The probability of failure is therefore given by

$$P_f(N) = \int_{\Omega_f^r} f_R(\boldsymbol{r}) P_{nd}(\boldsymbol{r},\ N)\ d\boldsymbol{r} \tag{3.7}$$

where Ω_f^r includes all $\boldsymbol{r}$ such that $g \leq 0$ (i.e. $N_f \leq N$). The probability of failure since the last inspection is given by

$$P_{fI}(N) = \int_{\Omega_{fI}^r} f_R(\boldsymbol{r}) P_{nd}(\boldsymbol{r},\ N)\ d\boldsymbol{r} \tag{3.8}$$

where Ω_{fI}^{r} includes all $\boldsymbol{r}$ such that $N_I<N_f\leq N$. Note that the computation of N_f is not influenced by the inspections, i.e. the failure surface $g(\boldsymbol{r})=0$ is not influenced by in-service inspections. Rather, it is the integrands in Eqs. (3.7) and (3.8) which incorporate the effect of inspections on failure probability.

3.2. Evaluation of the Integral for Failure Probability

The integrals in Eqs. (3.7) and (3.8) differ from that which arises in standard FORM in that the integrands have been multiplied by the non-Gaussian function $P_{nd}(\boldsymbol{r},N)$ and, therefore, the integration technique must be modified to accurately integrate the functions. A simple modification of the standard FORM integration procedure is introduced here for the evaluation of the integral in Eq. (3.7). As in standard FORM, the failure surface is approximated by a tangent hyperplane at the most likely failure point, $\boldsymbol{r}_d$ (the so-called design point). The sharp variation of $P_{nd}(\boldsymbol{r},N)$ in the direction of the gradient of g prevents the direct evaluation of the integral via the standard normal cumulative distribution function, as in Eq. (2.6). Nevertheless, we wish to maintain the essential structure of the FORM integration procedure and thus it is convenient to discretize the domain Ω_f^r into subdomains as shown in Fig. 2. By approximating $P_{nd}(\boldsymbol{r},N)$ as constant over each subdomain we obtain

$$P_f(N) \approx \sum_{j=1}^{n_s} \left[\bar{P}_{nd}^{j} \int_{\Omega_j} f_R(\boldsymbol{r})\, d\Omega \right], \tag{3.9}$$

where n_s is the number of subdomains and $\bar{P}_{nd}^{j}$ is the approximation of $P_{nd}(\boldsymbol{r},N)$ in the subdomain Ω_j. The remaining integrands $f_R(\boldsymbol{r})$ are Gaussian, so the standard cumulative normal function Φ is useful for "first order" approximations of these integrals. Thus, Eq. (3.9) leads to approximations of the form

$$P_f^I(N) = \sum_{j=1}^{n_s} \left\{ \bar{P}_{nd}^{j} \left[\Phi(-|\boldsymbol{r}|_j) - \Phi(-|\boldsymbol{r}|_{j+1}) \right] \right\} + \bar{P}_{nd}^{n_s} \Phi(-|\boldsymbol{r}|_{n_s}), \tag{3.10}$$

where $\boldsymbol{r}_j$ is the integration point on the surface of the subdomain Ω_j as shown in Fig. 2. In this numerical integration scheme, the design point is taken as the first integration point, i.e., $\boldsymbol{r}_1 = \boldsymbol{r}_d$. Subsequent integration points are found by

$$\boldsymbol{r}_j = \left[1 + (j-1)\delta\right] \boldsymbol{r}_d, \tag{3.11}$$

where $\boldsymbol{r}_j$ is the position of the j^{th} integration point and δ is the desired step size for the integration. The number of subdomains, the magnitude of δ, and the location, $\boldsymbol{r}_{n_s}$ of the last integration point depend on the

accuracy desired and can be deduced through numerical experimentation and comparison with known solutions. A non-uniform subdomain discretization can be used in place of Eq. (3.11) if desired.

3.3 Location of Design Points

In standard applications of FORM, the most likely failure point can be shown to be the closest point to the origin on the surface g=0 through the use of Lagrange multipliers (Ang and Tang 1984). The approximation of the failure surface as a tangent hyperplane at the design point leads to the first order approximation in Eq. (2.6). In the present application of FORM with in-service inspections, the integrand in Eq. (3.7) contains the non-Gaussian variable $P_{nd}(\boldsymbol{r},N)$ and the most likely failure point is not in general the closest point to the origin on g=0. The question then arises as to which point provides the most appropriate first order approximation to the failure surface, i.e. where to locate the design point. One possibility is to take the closest point to the origin on g=0 as in standard FORM. However, due to variations in $P_{nd}(\boldsymbol{r},N)$ along the surface g=0, an alternative point is suggested which will maximize the integrand in Eq. (3.7).

A procedure for locating the design point at the most likely failure point on g=0 is introduced here. By suitable choice of parameters, the algorithm can also be used to locate the design point at the closest point to the origin. Consider β such that

$$\Phi(-\beta) = P_{nd}(\boldsymbol{r}, N)\Phi(-|\boldsymbol{r}|). \tag{3.12}$$

The design point is the point on the surface of constant g which will minimize β (or maximize the product $P_{nd}(\boldsymbol{r},N)\Phi(-|\boldsymbol{r}|)$). Typically, the variation in $P_{nd}(\boldsymbol{r},N)$ is small in the direction of constant g and the design point and the closest point are nearly coincidental. However, some problems do show a significant difference. The Rackwitz algorithm (Rackwitz and Fiessler, 1978) can be used to find the design point for standard FORM, but this algorithm can be non-convergent for high values of β if the failure surface is not relatively flat. A variation of the Rackwitz algorithm which corrects for this problem and has been generalized for use with both standard and augmented FORM is presented in the Appendix.

4. NUMERICAL EXAMPLES

4.1. Edge Crack

We first consider the fatigue of an edge crack in a semi-infinite plate to investigate the accuracy of the augmented FORM based on comparisons with Monte Carlo simulations (MCS). It is assumed that the cracks propagate according to the Paris model (Paris and Erdogan, 1963)

$$\frac{da}{dN} = D(\Delta K)^m \tag{4.1}$$

where da/dN is the rate of crack growth, D and m are material parameters, and ΔK is the amplitude of the stress intensity factor. The stress intensity factor range for an edge crack of length a, is given by $\Delta K = 1.12\sigma(\pi a)^{1/2}$ where σ is the amplitude of the applied stress. Using this relation, Eq. 4.1 can be integrated to obtain the number of cycles for a crack of initial length a_i to grow to a crack of length a_f

$$N_f = \frac{a_f^{1-\frac{m}{2}} - a_i^{1-\frac{m}{2}}}{D(1-\frac{m}{2})(1.12\sigma\sqrt{\pi})^m}, \quad (m \neq 2) \tag{4.2}$$

$$N_f = \frac{\ln(a_f / a_i)}{\pi D(1.12\sigma)^2}, \quad (m=2). \tag{4.3}$$

The material is taken to be ingot 304 stainless steel with fracture toughness K_{Ic} = 48 MPa $\sqrt{\text{m}}$. The crack is cyclically loaded in tension-tension fatigue with an R -ratio of 0 and remote applied stress amplitude of σ = 250 MPa. Motivated by the experimental findings of McGuire (1993)*, the initial crack size distribution is taken to be lognormal with mean 0.1mm and standard deviation 0.033mm. The quantity m-1 is also taken to be lognormal with mean 2.67 and standard deviation 0.75. The coefficient D and the exponent m are also found to be functionally related as $\log D = -1.50m - 7.29$ - the units of D are m/cycle/(MPa$\sqrt{\text{m}}$)^m.

It is assumed that the probability of detecting an existing crack of length a upon inspection is (Palmberg et al., 1987)

$$POD(a) = \frac{\alpha a^\beta}{1+\alpha a^\beta}, \tag{4.4}$$

* The experimental data collected by McGuire (1993) are for fatigue crack growth from a hole in a tension-loaded bar. The statistical data obtained for this configuration are not directly transferable to the edge crack configuration, but do provide a reasonable representation of fatigure crack growth in this material.

where the parameters α and β depend on the inspection technique.

Figure 3 shows a comparison of augmented FORM and MCS results with evenly-spaced inspections modeled at $2.25\text{x}10^5$, $2.75\text{x}10^5$, $3.25\text{x}10^5$, and $3.75\text{x}10^5$ cycles. Monte Carlo results obtained using 10 million realizations are not very dependable for $P_f(N)$ below about $2\text{x}10^{-6}$. To obtain dependable MCS results, the POD curve A in Fig. 4 is used (α=0.0032 mm$^{-\beta}$, β=3.5) to yield probabilities of failure greater than $2\text{x}10^6$. The integration over the failure space is performed using the integration technique presented in Section 3.2 with n_s=100 and δ=0.01. As can be seen from the figure, excellent agreement is obtained between the two methods.

In a fatigue reliability setting, it is generally desirable to have failure probabilities much lower than those in Fig. 3. The probability of failure can be kept below a desired level by scheduling inspections at uneven intervals as well as improving the probability of detection through better NDE inspection techniques. Fig. 5 shows results for inspections modeled at $2.25\text{x}10^5$, $2.55\text{x}10^5$, $3.15\text{x}10^5$, and $2.75\text{x}10^5$ cycles and using the POD curve B in Fig. 4 (α=1.0 mm$^{-\beta}$, β=3.0) and using the same integration parameters for Eq. (3.11) as before (n_s=100, δ=0.01). Using this inspection schedule and POD relation, the peak probability of failure is kept below 10^{-5}. The augmented FORM and MCS estimates are in close agreement; however, as previously stated, MCS results are not very dependable for $P_f(N)$ below about $2\text{x}10^{-6}$.

4.2. Semi-Elliptical Surface-Breaking Crack

For complicated component geometries and crack shapes, a closed form expression for fatigue life is generally not available. This requires that the fatigue life for each realization of random variables $\boldsymbol{r}$ be determined by numerical integration, with the stress intensity factors updated as crack growth is simulated. This makes MCS infeasible for studies of extreme reliabilities. The augmented FORM requires the consideration of relatively few realizations, so these analyses are feasible when parameterizations or interpolation schemes for the stress intensity factors are available (see Newman and Raju 1986, for example).

A semi-elliptical surface-breaking crack in a plate as shown in Fig. 6 is considered, with the dimensions (in mm) h=b=5.0, t=2.5. It is assumed that there are no initial cracks in the component. Instead, a random distribution of the cycles to initiation, N_{init}, of a crack of depth 80μm is considered. It is assumed the crack remains planar and semi-elliptical as it propagates. Post-initiation crack growth is modeled by applying the Paris law to the crack depth, a, and half crack width, c

$$\frac{da}{dN} = D(\Delta K_A)^m \tag{4.5a}$$

$$\frac{dc}{dN} = D(\Delta K_C)^m \tag{4.5b}$$

Failure is assumed to correspond to the crack reaching a critical depth, a_f.

The stress intensity factors at points A and C, parameterized according to Newman and Raju (1986), are given by

$$K_A = S_t(\pi a/Q)^{1/2} F_s^A \tag{4.6a}$$

$$K_C = S_t(\pi a/Q)^{1/2} F_s^C, \tag{4.6b}$$

where S_t is the applied tensile stress, Q is the shape factor for an ellipse, and F_S is a boundary correction factor.

For this example, the initial crack length (a_i) is taken to be a deterministic variable at a_i=80 μm and the initial half crack width (c_i) is taken as c_i=1.1a_i. The maximum allowable crack length, a_f, is taken as a_f= 1.25 mm, which is 50% of the plate thickness.

The time required for a crack to reach the initiation depth, N_{init}, is taken to be a lognormally-distributed random variable with mean 10^6 and standard deviation $0.5\text{x}10^6$. The stress amplitude (S_t) is taken to be a normally distributed random variable with mean 250 MPa and standard deviation 7.5 MPa. The distributions for m and D are the same as in the previous example. The POD for the inspection technique considered in this example is shown in curve C in Fig. 4 (α=100 mm$^{-\beta}$ and β=5).

Augmented FORM results are shown in Figs. 7 and 8 for probability of failure and probability of failure since the last inspection, respectively. Note that the entire set of data points shown was obtained with less than two minutes of CPU on an HP 9000 series 750 computer. Inspections were simulated at $4.2\text{x}10^5$, $5.1\text{x}10^5$, $5.8\text{x}10^5$, and $6.5\text{x}10^5$. As in the last example, the inspections times have been adjusted so the probability of failure peaks at about 10^{-5} before an inspection is performed.

Note that the reliability results are given over a range of fatigue lives considerably below the mean value of N_{init}. This shows that even though the initiation times are usually great, it is the few relatively short initiation times which are important to the reliability and to the scheduling of inspections.

5. SUMMARY AND DISCUSSION

A technique to incorporate periodic in-service inspections in a FORM analysis of fatigue life has been presented. The attractive feature of FORM is preserved in that relatively few realizations in the random variable space need to be considered. This is especially important when fatigue reliability of complex components is studied, since closed form expressions for the fatigue life are not available and numerical integration is required to determine the fatigue life corresponding to a combination of random variables.

Previous applications of FORM to multiple inspection intervals have required that the probability density function for the crack length be determined at an initial state as well as after each inspection. The augmented FORM only requires knowledge of the initial distribution of crack lengths (or the distribution of cycles to crack initiation), which is a significant advantage. Recharacterizing the crack length distribution after each inspection requires the consideration of a great deal of realizations. Therefore, the advantage of FORM is greatly diminished, if not lost, if the crack length distribution must be recharacterized at various stages of the fatigue life.

Demonstrations of the augmented FORM were given for two components to show the accuracy and versatility of the method. The first component had a simple configuration which allowed comparisons with Monte Carlo simulations. These comparisons showed that the augmented FORM yields accurate probability of failure estimates. In the second component, the augmented FORM was shown to be efficient for even complex components when other methods, such as MCS and standard FORM, were computationally infeasible.

The method has also been shown to be an effective tool for scheduling inspection times based on a maximum probability of failure. The probability of failure was kept below a specified level by performing non-uniform inspections, rather than evenly spaced inspections. This and related aspects of the method are subjects of our ongoing research in this area.

ACKNOWLEDGMENTS

This work was partially supported by the National Institute for Standards and Technology through a subcontract with Iowa State University and partially supported by the Federal Aviation Administration. Helpful discussions with Dr. Al Berens, University of Dayton Research Institute, are gratefully acknowledged.

REFERENCES

Ang, A.H., and W.H. Tang. *Probability Concepts in Engineering Planning and Design*, 1st Edit., Vol. II. Wiley and Sons, New York (1984).

Berens, A.P., J.G. Burns, and J.L. Rudd. Risk Analysis for Aging Aircraft Fleets. In *Structural Integrity of Aging Airplanes*. ed. S.N. Atluri, S.G. Sampath, and P. Tong. Springer-Verlag, New York (1991).

Harkness, H.H., T.B. Belytschko, and W.K. Liu. Finite element reliability analysis of fatigue life. *Nucl.Engng Des.* **133**, 209-224 (1992).

Harkness, H.H. Computational Methods for Fracture Mechanics and Probabilistic Fatigue. Ph.D. diss., Northwestern University (1993).

McGuire, S.M. Quantitative Measurement of Fatigue Crack Initiation and Propagation in 304 Stainless Steel as Related to Design and Nondestructive Evaluation. Ph.D. diss., Northwestern University (1993).

Newman, J.C. Jr., and I.S. Raju. Stress intensity factor equations for cracks in three dimensional finite bodies subjected to tension and bending loads. In *Computational Methods in the Mechanics of Fracture*, ed. S.N. Atluri, 312-334. North-Holland, New York (1986).

Palmberg, B., A.F. Blom, and S. Eggwertz. Probabilistic damage tolerance analysis of aircraft structures. In *Probabilistic Fracture Mechanics and Reliability*. ed. J.W. Provan. Martinus Nijhoff, Boston (1987).

Paris, P.C., and F. Erdogan. A critical analysis of crack propagation laws. *J. Bas Engng*, **85**, 528-534 (1963).

Rackwitz, R., and B. Fiessler. Structural reliability under combined random load sequences. *Computers and Structures*. **9**, 489-494 (1978).

Rahman, S., and R. Rice. Assessment of the reliability of the commercial aircraft fleet considering the potential adverse effects of multiple repairs and multiple site damage, preliminary technical interchange report for U.S. DOT/FAATC Aging Aircraft Program (1992).

Rosenblatt, M. Remarks on a Multivariate Transformation. *Annals of Mathematical Statistics*. **23**, 470-472 (1952).

APPENDIX: ALGORITHM TO LOCATE DESIGN POINTS

A variation on the Rackwitz algorithm (Rackwitz and Fiessler, 1978) is presented in the following four steps (Harkness, 1993):

1) define failure function $G(\boldsymbol{x})$, initialize iteration count: v=0; estimate design point coordinates r_i^0; transform r_i^0 to x_i^0.

2) evaluate g, $\frac{\partial \beta}{\partial r_i}$, and $\frac{\partial G}{\partial r_i}$ at x_i^v, r_i^v and compute:

$$I_i = -\lambda \frac{\partial G}{\partial r_i} \Big/ \frac{\partial \beta}{\partial r_i}, \text{ where } \lambda = |\nabla_r \beta| / |\nabla_r g|$$

3) increment iteration count: $v=v+1$; update r_i values in two steps:

a) $r_i^{temp} = r_i^{v-1} - (G - G^*) \frac{\partial G}{\partial r_i} \Big/ (\nabla_r G)^2$; adjusts magnitude of $\boldsymbol{r}$

b) $r_i^v = r_i^{temp} (\xi + (1-\xi) I_i)$, $0<\xi<1$; adjusts direction of $\boldsymbol{r}$

4) transform r_i^v to x_i^v; check for convergence:

If not converged, go to step 2.
If converged, design point found; reliability index $\beta_d = |\boldsymbol{r}^v|$.

This algorithm minimizes β on <u>any</u> surface of constant g (equal to g^*). Other distinctions between this algorithm and the Rackwitz algorithm are:

1) $G=G^*$ is not enforced on each iteration. Instead, step 3a just brings $\boldsymbol{r}^v$ toward the limit surface. In practice, $G \approx G^*$ after several iterations (i.e., after $v>4$) with the algorithm presented above.

2) The iteration parameter ξ is introduced to avoid the large angular corrections in $\boldsymbol{r}^v$ which lead to non-convergence.

An intermediate value of the iteration parameter, such as $\xi=0.7$, is recommended. For practical purposes, convergence can be assumed to have occurred when each of the standardized variables changes by less than 0.01 in an iteration. Convergence is typically achieved within ten to twenty iterations with this algorithm, and lack of convergence is uncommon.

The algorithm can be used to find design points for standard or augmented FORM. The algorithm calls for partial derivatives of $\beta=|\boldsymbol{r}|$ and G with respect to r_i. For standard FORM, these derivatives are given by

$$\frac{\partial \beta}{\partial r_i} = \frac{r_i}{\beta} \tag{A.1}$$

$$\frac{\partial G}{\partial r_i} = \frac{\partial G}{\partial x_i} \frac{\partial x_i}{\partial r_i}. \tag{A.2}$$

If $G = Nf - N$ and the desired service life is deterministic, then

$$\frac{\partial G}{\partial x_i} = \frac{\partial N_f}{\partial x_i} \tag{A.3}$$

and

$$\frac{\partial x_i}{\partial r_i} = \sigma_i^N, \tag{A.4}$$

where σ_i^N are the equivalent normal standard deviations in the Rosenblatt transformation (see Ang and Tang, 1984). With these substitutions,

$$\frac{\partial G}{\partial r_i} = \frac{\partial N_f}{\partial x_i}\sigma_i^N. \tag{A.5}$$

For augmented FORM, the derivatives of β with respect to r_i are modified to account for the affect of the $P_{nd}(r,N)$ function on the design points (see Section 3.3). The derivatives can now be calculated as

$$\frac{\partial \beta}{\partial r_i} = \frac{r_i}{\beta} + \frac{R}{\beta}\frac{\partial R}{\partial r_i} \tag{A.6}$$

where $R = \sqrt{\beta^2 - |r|^2}$. The derivatives of the "augmented component" R can be calculated using finite differences.

For both standard and augmented FORM, $|\nabla_r \beta| = 1$.

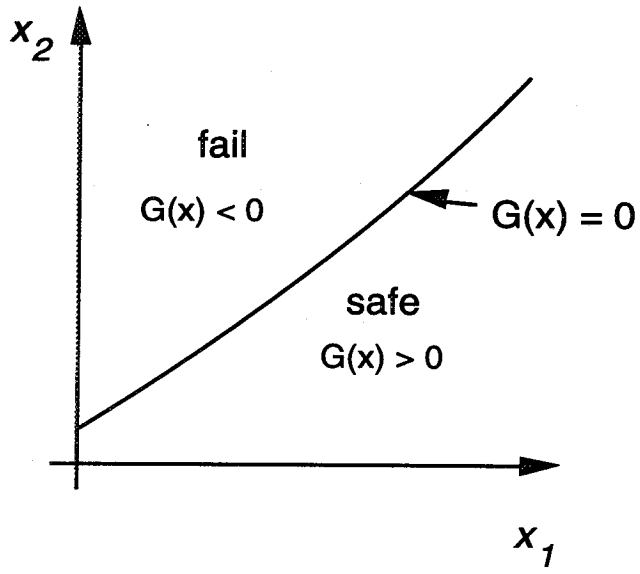

Figure 1a. Failure surface in original space

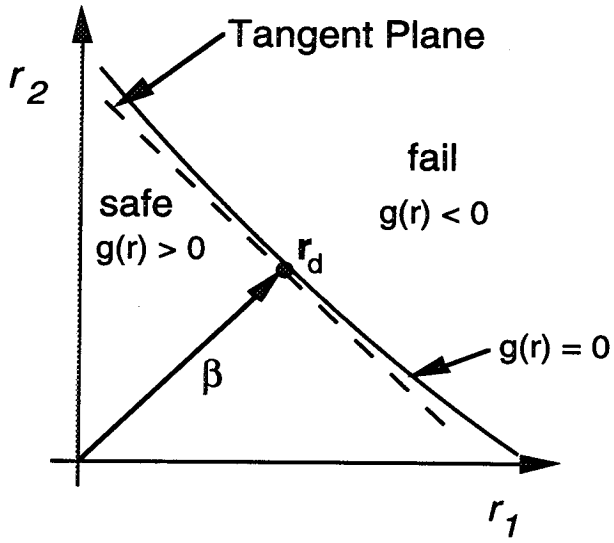

Figure 1b. Failure surface in standardized space

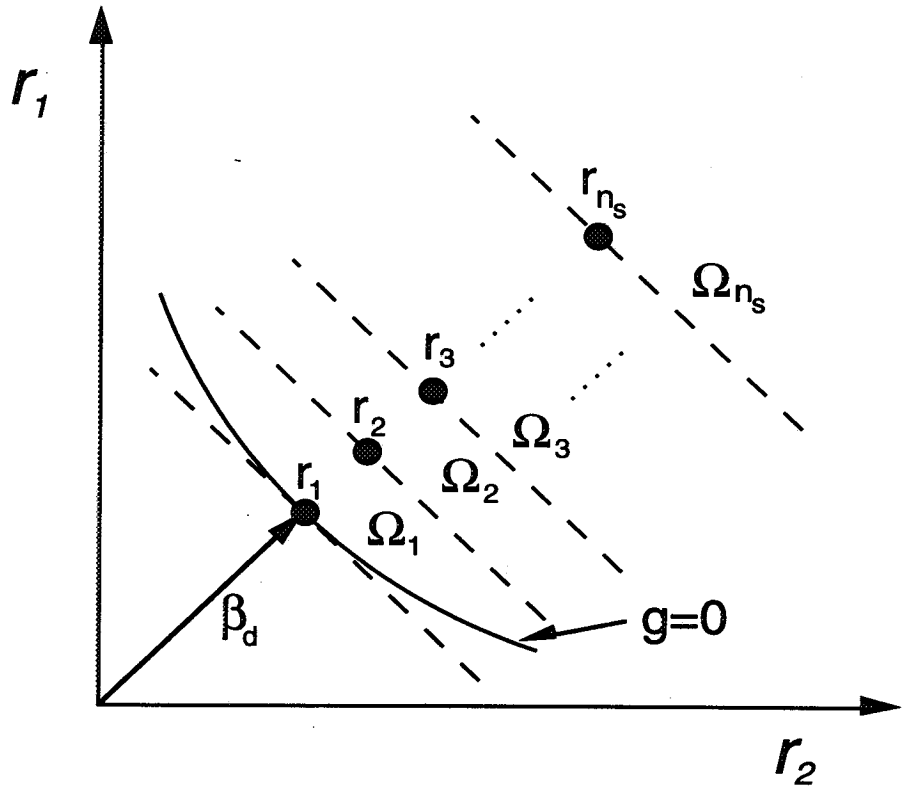

Figure 2. FORM integration scheme

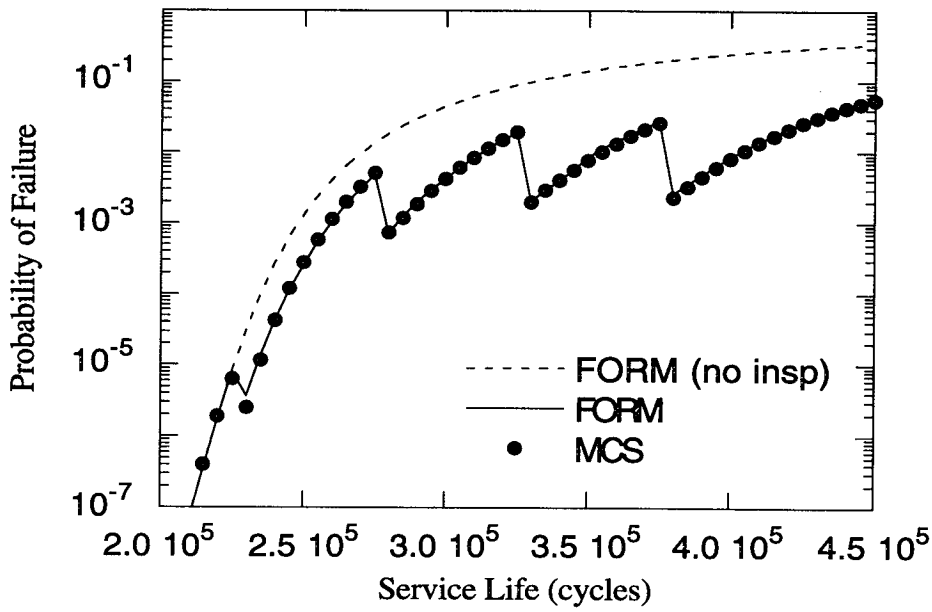

Figure 3. Probability of Failure for test case with and without inspections.

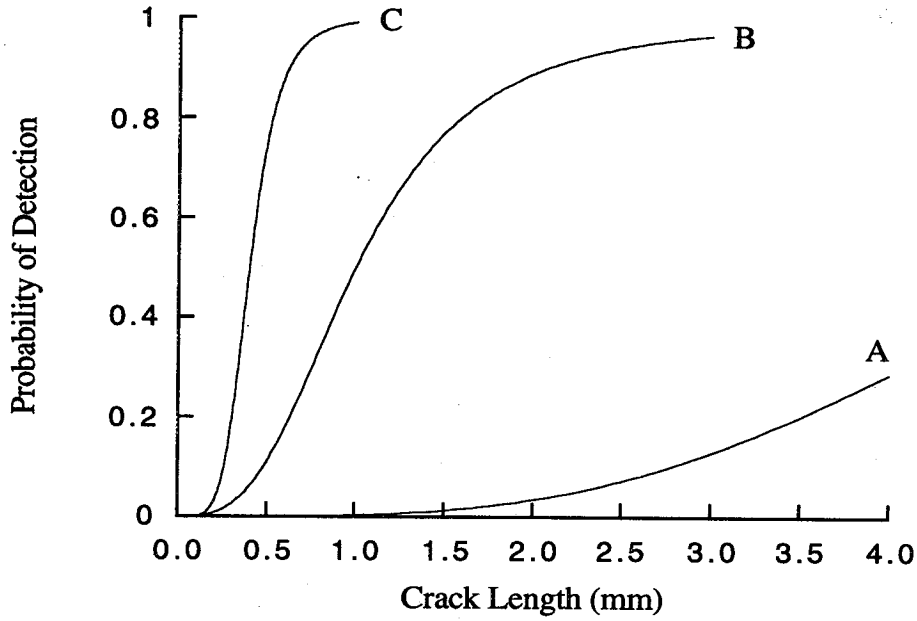

Figure 4. Probability of detection curves (A: α=0.0032 mm$^{-\beta}$, β=3.5; B: α=1 mm$^{-\beta}$, β=3; C: α= 100mm$^{-\beta}$, β=5)

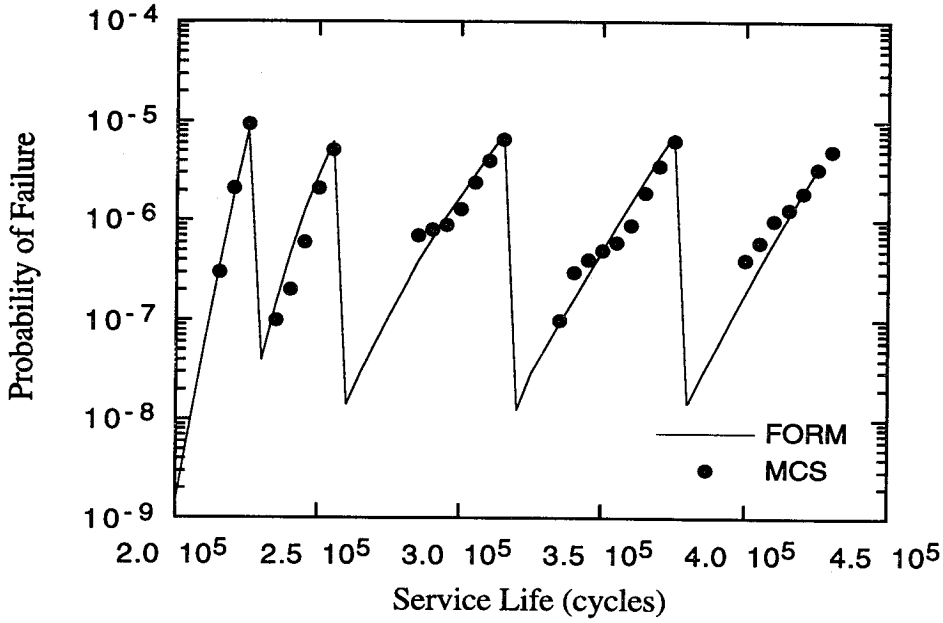

Figure 5. Results for edge crack using augmented FORM and uneven inspection intervals.

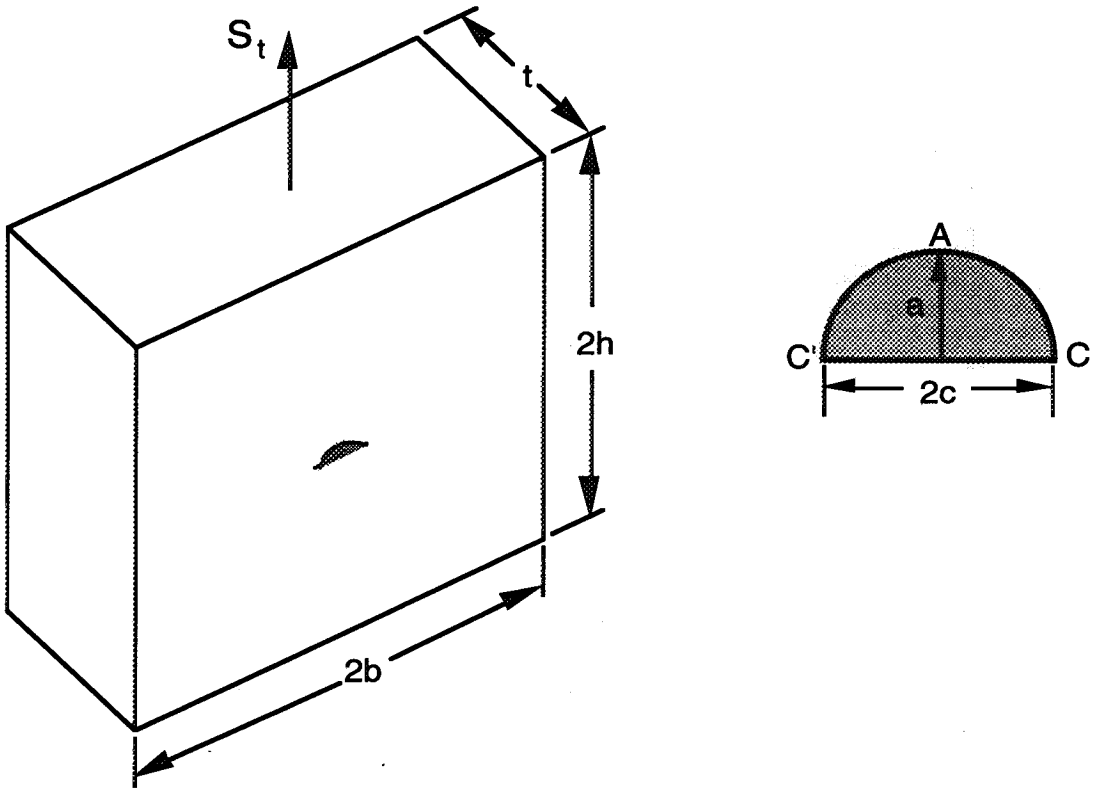

Figure 6. Rectangular plate with surface-breaking semi-elliptical crack.

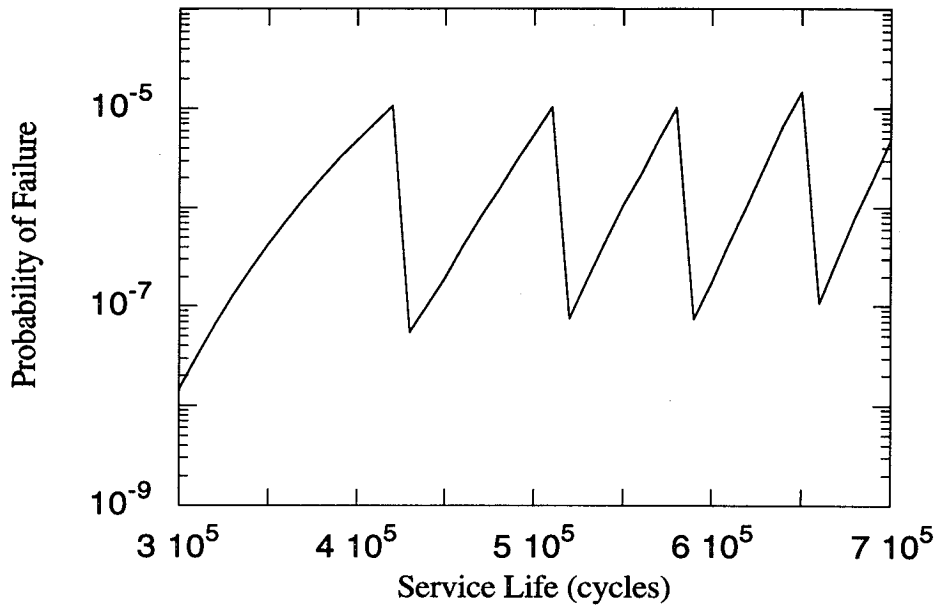

Figure 7. Probability of failure for surface-breaking crack in a plate.

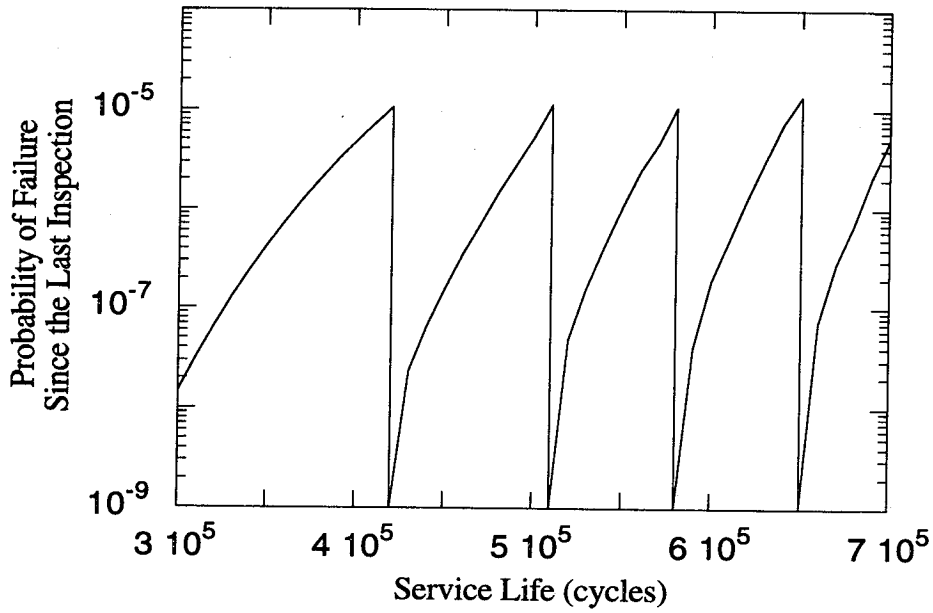

Figure 8. Probability of failure since the last inspection for surface-breaking crack in a plate